Journal of Physiology (1997), **498.3**, *pp.*717–727

Variation in expression of the outer hair cell P2X receptor conductance along the guinea-pig cochlea

N. P. Raybould and G. D. Housley

Department of Physiology, School of Medicine, University of Auckland, Private Bag 92019, Auckland, New Zealand

1. Whole-cell patch-clamp recordings were used to determine the variation in the P2X receptor conductance, activated by extracellular ATP, in outer hair cells (OHCs) isolated from each of the four turns of the guinea-pig cochlea.

2. In standard solution (containing 1·5 mM Ca^{2+}) slope conductances were determined in OHCs of known origin from current–voltage relationships obtained from voltage ramps applied between −100 and +50 mV. Membrane conductance throughout this voltage range was greatest in OHCs originating from the basal (high frequency encoding) region of the cochlea. This gradient in OHC conductance from apex to base of the cochlea can be attributed to variation in expression of both a negatively activated K^+ conductance and a TEA-sensitive outwardly rectifying K^+ conductance. OHC slope conductance measured about a membrane potential of −75 mV increased from a mean of 33·5 nS in the apical region (turn 4) to 96·8 nS in the basal region (turn 1) of the cochlea.

3. Removal of external Ca^{2+} reduced OHC conductance by an average of 25%, reflecting a Ca^{2+} dependence of the background conductances in these cells. In zero external Ca^{2+} the mean slope conductance measured at −75 mV in the apical turn was 25·0 nS compared with 73·8 nS in the basal turn.

4. In Ca^{2+}-free solution both 2 mM and 4 μM ATP produced inward currents that were progressively larger in OHCs originating from more basal regions of the cochlea. The steady-state inward current elicited by 2 mM extracellular ATP increased from −1·44 to −3·26 nA for turns 4 and 1, respectively.

5. The P2X receptor conductance was determined between −100 and +50 mV by comparing voltage ramps in the presence and absence of extracellular ATP in Ca^{2+}-free solution. The conductance was inwardly rectifying with a reversal potential close to 0 mV. Measured close to the resting membrane potential of the cells (−75 mV), 2 mM ATP elicited an average 300% increase in conductance in parallel with the systematic increase in background conductance which occurs in OHCs originating from the more basal regions of the cochlea. The conductance at −75 mV activated by 2 mM ATP increased from a mean of 59·6 nS in turn 4 OHCs to a mean of 166·2 nS in turn 1 OHCs. The conductance activated by 4 μM ATP was also greater in the basal turn OHCs (45·3 nS) than in the apical region OHCs (5·9 nS).

6. The number of ATP-gated ion channels on individual OHCs, presumed to be localized to the stereocilia, increases from approximately 6000 in turn 4 cells to 16 500 in turn 1 cells, based on estimates of unitary conductance and average maximum ATP-activated OHC conductance (2 mM ATP).

Adenosine 5′-triphosphate (ATP), familiar as the primary energy source for cellular metabolism, has a wide variety of neural and humoral signalling roles (Burnstock, 1981, 1995; Gordon, 1986). These roles include many of the sensory modalities and are mediated by ATP-gated ion channels assembled from P2X receptor subunits and G-protein-coupled P2Y receptors (Thorne & Housley, 1996).

Involvement of extracellular ATP in cochlear physiology was first suggested by ATP activation of an inwardly rectifying non-selective cation conductance and ATP-induced elevations in $[Ca^{2+}]_i$ in isolated cochlear outer hair cells (OHCs) (Nakagawa, Akaike, Kimitsuki, Komune & Arima, 1990; Ashmore & Ohmori, 1990; Ashmore, Housley & Kolston, 1992). Extracellular ATP may act as an endolymph-borne

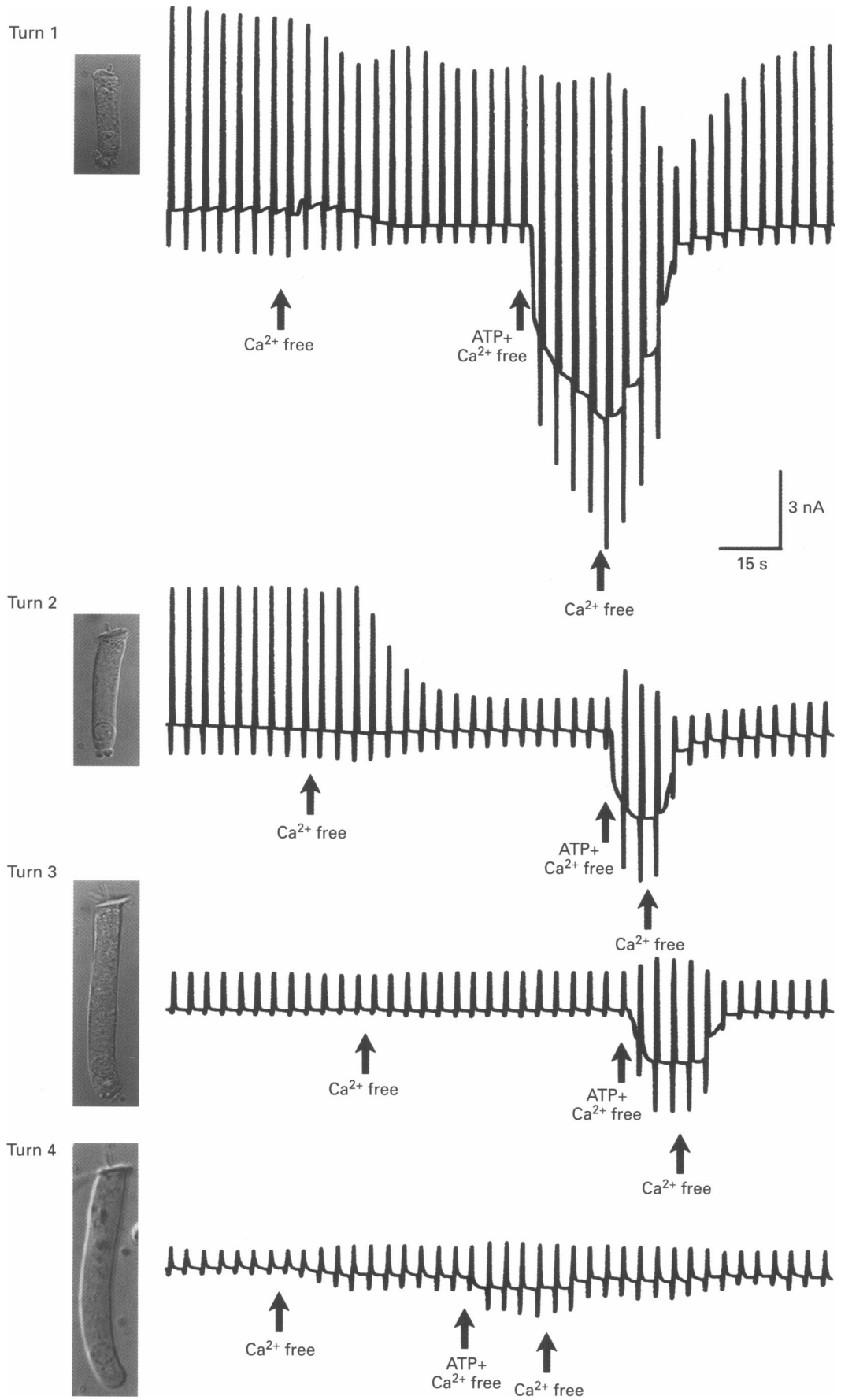

Figure 1. For legend see facing page.

humoral factor regulating hearing function. ATP is present in endolymph (Muñoz, Thorne, Housley & Billett, 1995*a*), where it has a suppressive effect on endocochlear potential and the cochlear microphonic (Muñoz, Thorne, Housley, Billett & Battersby, 1995*b*) and operates via a number of different receptor subtypes and pathways (Liu, Kozakura & Marcus, 1995; Mockett, Bo, Housley, Thorne & Burnstock, 1995; Thorne & Housley, 1996). Additionally, ATP-gated ion channels are localized to the endolymphatic surface of the inner and outer hair cells and Hensen cells (Housley, Greenwood & Ashmore, 1992; Housley, Greenwood, Mockett, Muñoz & Thorne, 1993; Mockett, Housley & Thorne, 1994; Housley, Connor & Raybould, 1995*a*; Sugasawa, Erostegui, Blanchet & Dulon 1996*a*,*b*; Thorne & Housley, 1996). Recently reverse transcriptase-polymerase chain reaction and riboprobe-based *in situ* hybridization data (Housley, Greenwood, Bennett, Luo & Ryan, 1995*b*; Housley, Greenwood, Bennett & Ryan, 1995*c*) have suggested that in cochlear hair cells it is the $P2X_2$ receptor subunits which assemble to form ATP-gated ion channels (Thorne & Housley, 1996).

Guinea-pig cochlear OHCs exhibit an increased membrane conductance in the basal (high frequency responding) region of the cochlea compared with the apical region (Housley & Ashmore, 1992). Preliminary studies of the response of OHCs to extracellular ATP under voltage-clamp conditions suggested that a similar gradient in ATP-activated non-selective cation conductance with respect to OHC position in the organ of Corti may also exist (Housley *et al.* 1995*a*). The present study provides evidence for a systematic increase in the ATP-activated P2X receptor conductance towards the base of the cochlea, proportional to the variation in the background conductance, but outstripping it by a factor of three.

METHODS

Isolation of guinea-pig cochlear OHCs and whole-cell patch-clamp recordings were made as previously described (Housley *et al.* 1992). All experiments were carried out with the approval of the University of Auckland Animal Ethics Committee. Briefly, adult guinea-pigs (200–800 g body weight, either sex, both pigmented and albino) were killed by rapid cervical dislocation, the temporal bones excised to allow access to the auditory bulla and the cochlea exposed. The cochlea, fused to the bulla, was placed in an artificial perilymph (standard) solution (mM: NaCl, 152; KCl, 4·0; $CaCl_2$, 1·5; $MgCl_2$, 1·0; NaH_2PO_4, 2·0; and Na_2HPO_4, 8·0; pH 7·25, corrected with 2 mM NaOH). Osmolarity (approximately 315 mosmol l^{-1}) was measured using a vapour pressure osmometer (Wescor 5500, Logan, UT, USA). The otic capsule was opened, allowing removal of the sensory epithelium (organ of Corti) attached to the modiolus. OHCs were isolated by micro-dissecting a selected turn of the organ of Corti; from turn 1 of the cochlea (corresponding to the region transducing 45–6 kHz) to turn 4 (low frequency, < 200 Hz apical region; Table 1; Pujol, Lenoir, Ladrech, Tribillac & Rebillard, 1992). A selected turn of the organ of Corti was incubated for 10 min in standard extracellular solution containing 250 μg ml^{-1} trypsin (Sigma), then rapidly triturated to dissociate the OHCs. Cells were placed in a laminar flow bath (100 μl) mounted on the stage of a Nikon TMD inverted microscope equipped with Nomarski Differential Interference Contrast optics. Exchange of all solutions (> 850 μl min^{-1}) was achieved using a peristaltic pump (Minipuls 2, Gilson, France).

OHCs were visualized and the following morphological features were used to determine quality: preservation of cylindrical uniformity with close juxtaposition of the cell membrane to the basally positioned nucleus; birefringence of the membrane; absence of Brownian motion; and intact stereocilia. Images were captured by video camera (Ikegami ICD 42E, CCD, Japan) and recorded continuously by sVHS recorder (Panasonic AG 7330, Japan). Cell length and width were determined *post hoc* by image analysis (Image Pro Plus, version 1.0, Media Cybernetics, Silver Spring, MD, USA) using an 8-bit video frame grabber (ITEX, Woburn, MA, USA). All measurements of cell dimensions (resolution, 0·3 μm) were corrected for aspect ratio distortion.

Recording electrodes (2–5 MΩ; filamented borosilicate glass, Clark Electromedical GC120 TF-10, UK) filled with internal solution (mM: KCl, 150; $MgCl_2$, 2·0; NaH_2PO_4, 1·0; Na_2HPO_4, 8·0; EGTA, 0·5; $CaCl_2$, 0·01; and D-glucose, 3·0; pH 7·25, adjusted with 2 mM KOH, 305 mosmol l^{-1}) were placed in close contact with the baso-lateral wall of the OHCs. After obtaining a gigaseal, whole-cell recording configuration was attained by gentle suction and a brief hyperpolarizing voltage step (−130 mV, 1 s; after Hamill, Marty, Neher, Sakmann & Sigworth, 1981). Voltage clamp was controlled by a patch-clamp amplifier (Axopatch 200, Axon Instruments) using pCLAMP 5.0 control software (Axon Instruments) and interface (Tecmar TL 1, Labmaster Scientific Solutions, Solon, OH, USA). Experiments were performed on cells with stable current

Figure 1. Comparison of responses to extracellular ATP (2 mM) in OHCs isolated from each of the four turns of the guinea-pig cochlea

Chart record depicting chronological series of electrophysiological events in the current trace during the sequential superfusion of standard solution, Ca^{2+}-free solution, 2 mM ATP-containing, Ca^{2+}-free solution and Ca^{2+}-free washout. Repeated voltage ramps (1 s, −100 to +50 mV, 0·2 Hz), seen as bidirectional deflections in the current trace, were applied to OHCs voltage clamped at −60 mV to provide a measure of membrane conductance. In standard solution the greater conductance of the more basal OHCs (turns 1 and 2) is evidenced by the larger size of the inward and outward components of the current deflections. Removal of extracellular calcium produced shifts in the current baseline, indicating a change in V_z and reduction in both the peak inward and outward current components. The greatest reductions in conductance were recorded in OHCs from the more basal regions of the cochlea. Application of 2 mM ATP-containing, Ca^{2+}-free solution caused a rapid inward current and increase in the magnitude of the deflections in the current trace. The ATP-activated conductance varied systematically, being greatest in the more basal OHCs. Turn 1 cell length, 34·9 μm; turn 2 cell length, 47·3 μm; turn 3 cell length, 76·3 μm; turn 4 cell length, 83·5 μm.

Table 1. Relationship of OHC origin to cell length, membrane capacitance and membrane time constant

	Equivalent auditory range* (kHz)	Mean OHC length† (μm)	OHC length range† (μm)	C† (pF)	τ_{STD}† (ms)	τ_{CF}† (ms)	$\tau_{ATP\,(2mM)}$†† (ms)	$\tau_{ATP\,(4\mu M)}$††† (ms)
Turn 1	45–6	28·6 ± 1·1	17·7–37·2	15·2 ± 2·7	0·17 ± 0·03	0·30 ± 0·07	0·11 ± 0·03	0·11 ± 0·03
Turn 2	6–2·0	40·9 ± 1·2	28·9–58·6	19·1 ± 1·9	0·32 ± 0·04	0·41 ± 0·04	0·13 ± 0·02	0·17 ± 0·02
Turn 3	2·0–0·6	62·2 ± 3·1	33·9–80·4	28·0 ± 1·1	1·76 ± 0·52	1·54 ± 0·34	1·10 ± 0·52	0·99 ± 0·27
Turn 4	0·6–0·2	61·3 ± 2·3	44·6–83·5	28·8 ± 1·3	2·16 ± 0·56	2·08 ± 0·49	0·73 ± 0·21	0·97 ± 0·20

All values quoted are means ± S.E.M. * Auditory frequencies adapted from Pujol *et al.* (1992). † $n = 129$: turn 1, $n = 26$; turn 2, $n = 37$; turn 3, $n = 30$; turn 4, $n = 36$. †† $n = 72$: turn 1, $n = 10$; turn 2, $n = 16$; turn 3, $n = 20$; turn 4, $n = 26$. ††† $n = 55$: turn 1, $n = 18$; turn 2, $n = 17$; turn 3, $n = 10$; turn 4, $n = 10$. Abbreviations: STD, standard solution; CF, Ca^{2+}-free solution; ATP, ATP-containing, Ca^{2+}-free solution; τ, membrane time constant. $\tau = RC$, where R is $1/G_{-75mV}$ and C is membrane capacitance measured at −70 mV.

baselines and zero-current potentials (V_z) more negative than −50 mV. Application of a −10 mV voltage step (50 ms) from a holding potential (V_h) of −60 mV allowed calculation of series resistance, input resistance and cell capacitance from the capacitive charging transient (sampled at 30 kHz). Recordings were corrected for junction potential and > 95% series resistance-induced voltage error.

Continuously applied voltage ramps (1 s, −100 to +50 mV at 0·2 Hz) were used to quantify voltage-dependent conductances. Initial superfusion with standard solution was followed by superfusion with a Ca^{2+}-free solution ($MgCl_2$ substituted for the 1·5 mM $CaCl_2$). Ca^{2+}-free solution was used to prevent Ca^{2+} entry through ATP-gated ion channels causing secondary activation of Ca^{2+}-dependent conductances (Housley & Ashmore, 1992; Ashmore, 1994). A saturating 2 mM dose of ATP in the Ca^{2+}-free solution (pH 7·0) was then used to determine the maximum ATP-activated conductance. A second series of experiments used a concentration of ATP (4 μM; pH 7·2) below the 12 μM K_d (Mockett *et al.* 1994) for comparison. The ATP-activated current–voltage (I–V) profile was determined within 10 s of exposure to ATP by subtracting the control I–V relationship from that obtained in the presence of ATP. Conductances were measured about −75 and 0 mV by determining the current amplitude at ±15 and ±10 mV to these respective values. The resulting slope conductances were a robust measure of the current tangential to the reference values, particularly for analysis of large ATP-activated conductances. Significance was determined at the $P < 0·05$ level using the statistical package SYSTAT (Wilkinson, Leyland, SYSTAT, Inc., Evanston, IL, USA) to perform one-way ANOVA for comparison across all turns of the cochlea and Student's paired and unpaired t tests where appropriate. All values quoted are means ± S.E.M.

RESULTS

To investigate a possible position-dependent variation in ATP-activated conductance, whole-cell currents were recorded from OHCs isolated from each of the four turns of the guinea-pig cochlea; from the high frequency region at the base (turn 1) to apical regions transducing progressively lower frequencies. Upon patch rupture, cells voltage clamped at −60 mV typically exhibited an inward current that reversed to a small standing outward current over 1–2 min with equilibration of the pipette contents, consistent with the cells being initially depolarized. All OHCs studied demonstrated stable baseline currents with V_z more negative than −50 mV. The mean series resistance was 6·5 ± 0·2 MΩ, varying between 2·1 and 14·3 MΩ with no significant difference between turns. Cell capacitance, measured at −70 mV, varied between turns, ranging from a mean of 15·2 ± 2·7 pF in turn 1 to 28·8 ± 1·3 pF in turn 4 (Table 1).

Conductance in standard extracellular solution

OHCs superfused with standard solution demonstrated the systematic increase in conductance from base to apex of the cochlea (Figs 1 and 2) which has previously been attributed to the greater expression of a negatively activated K^+ conductance ($G_{K,n}$) (Housley & Ashmore, 1992). The I–V profile of OHCs from turns 3 and 4 showed a non-linear portion at potentials greater than approximately −35 mV, reflecting the outwardly rectifying TEA-sensitive K^+ conductance ($G_{K,TEA}$) (Housley & Ashmore, 1992).

In standard extracellular solution the mean V_z of all cells was −63·1 ± 0·6 mV with no significant difference across turns. Slope conductance about −75 mV systematically increased from a mean value of 33·5 ± 3·9 nS in turn 4 OHCs to 96·8 ± 7·4 nS in turn 1 (Fig. 3*A*). Slope conductance about 0 mV, used as an index of the combined activation of both $G_{K,n}$ and $G_{K,TEA}$, also increased systematically from 30·0 ± 3·2 nS in the apex to 76·4 ± 6·2 nS in the base (Figs 2 and 3*B*).

Conductance in Ca^{2+}-free solution

Superfusion of Ca^{2+}-free solution produced a significant depolarizing shift of 4·6 mV in V_z, to a mean of −58·5 ± 1·0 mV for cells from all turns. OHC conductance determined about −75 mV was significantly reduced by 17–30% across the four turns (Fig. 3), while the overall position-dependent

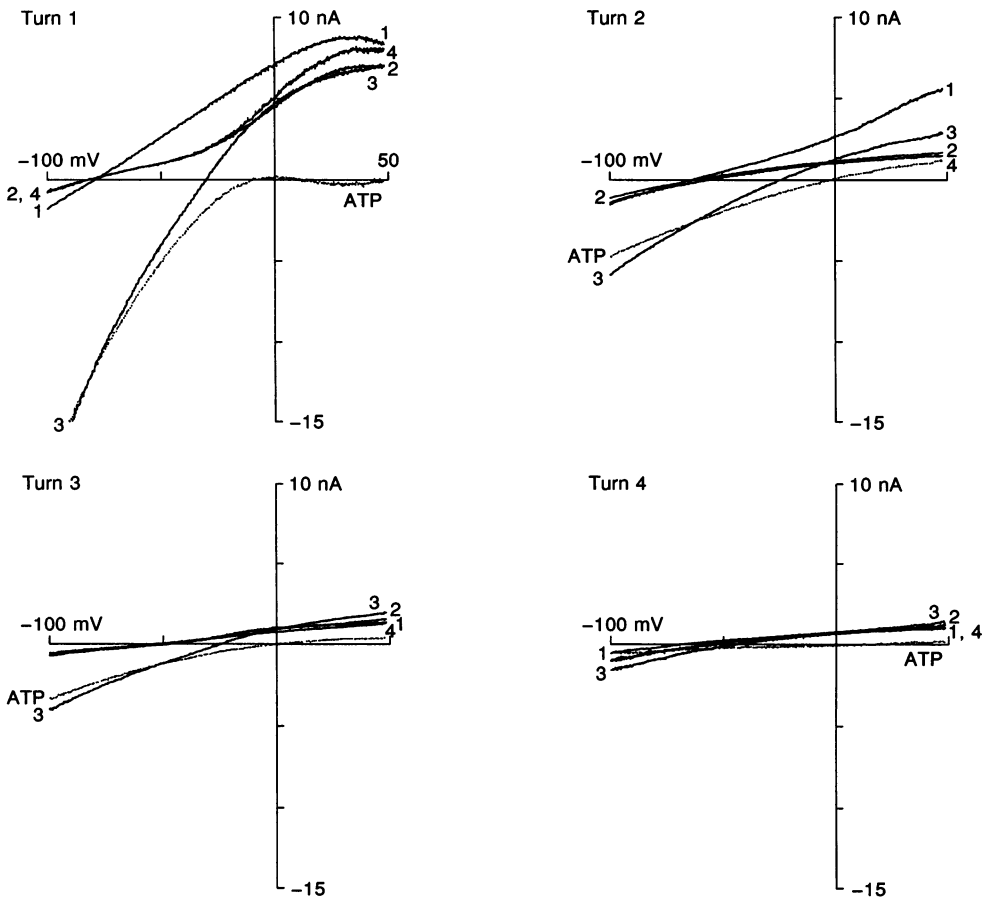

Figure 2. Details of *I–V* relationships (95% series resistance corrected) obtained from 1 s voltage ramps from −100 to +50 mV for OHCs isolated from the four turns of the cochlea shown in Fig. 1

Relationships are shown for five conditions: standard solution (1); Ca^{2+}-free solution (2); 2 mM ATP-containing, Ca^{2+}-free solution (3); Ca^{2+}-free wash (4); and net ATP (ATP). In standard solution slope conductance about −75 mV displayed a position dependence, being greatest in the most basal cell (turn 1 (T1) = 85·6 nS) and decreasing progressively in the more apical cells (turn 2 (T2) = 39·1 nS; turn 3 (T3) = 12·5 nS; turn 4 (T4) = 4·1 nS). A similar gradient was evident in slope conductance about 0 mV (T1 = 77·2 nS; T2 = 49·3 nS; T3 = 12·8 nS; T4 = 19·7 nS). Cells had V_z values of −78, −63, −53 and −55 mV, respectively. Superfusion of Ca^{2+}-free solution reduced both the inward and outward current components in a position-dependent manner (traces 2). Slope conductance about −75 mV was substantially reduced in the turn 1 cell (T1 = 36·8 nS) with progressively smaller changes in the more apical cells (T2 = 26·0 nS; T3 = 13·4 nS; T4 = 5·9 nS). Alterations in slope conductance about 0 mV in Ca^{2+}-free solution were variable owing to the change in shape of the *I–V* relationship, with an increase recorded in the turn 1 cell due to the development of an outward rectifier, whereas progressively smaller reductions in slope conductance occurred in more apical cells (T1 = 96·2 nS; T2 = 8·1 nS; T3 = 13·2 nS; T4 = 18·5 nS). Shifts in V_z were in either direction (T1 = −81 mV; T2 = −62 mV; T3 = −51 mV; T4 = −47 mV). Application of 2 mM ATP (in Ca^{2+}-free conditions) produced a progressively greater increase in slope conductance about −75 mV in the more basally positioned cells (traces 3: T1 = 291·3 nS; T2 = 87·4 nS; T3 = 60·8 nS; T4 = 8·0 nS) and a positive shift in V_z (T1 = −29 mV; T2 = −15 mV; T3 = −24 mV; T4 = −36 mV). Subtraction of the control (Ca^{2+}-free) data from the ATP-containing, Ca^{2+}-free data revealed the net inwardly rectifying ATP-gated currents, which reversed close to 0 mV (traces labelled ATP). These net ATP-activated conductances about −75 mV exhibited a clear dependence on turn of origin, decreasing progressively in the more apical cells (T1 = 254·6 nS; T2 = 61·4 nS; T3 = 47·4 nS; T4 = 2·1 nS). The inward rectification of the ATP-activated conductance resulted in smaller net slope conductances about 0 mV (T1 = 12·7 nS; T2 = 34·2 nS; T3 = 15·0 nS; T4 = 4·2 nS; ATP trace was obtained by subtracting traces 2 from traces 3).

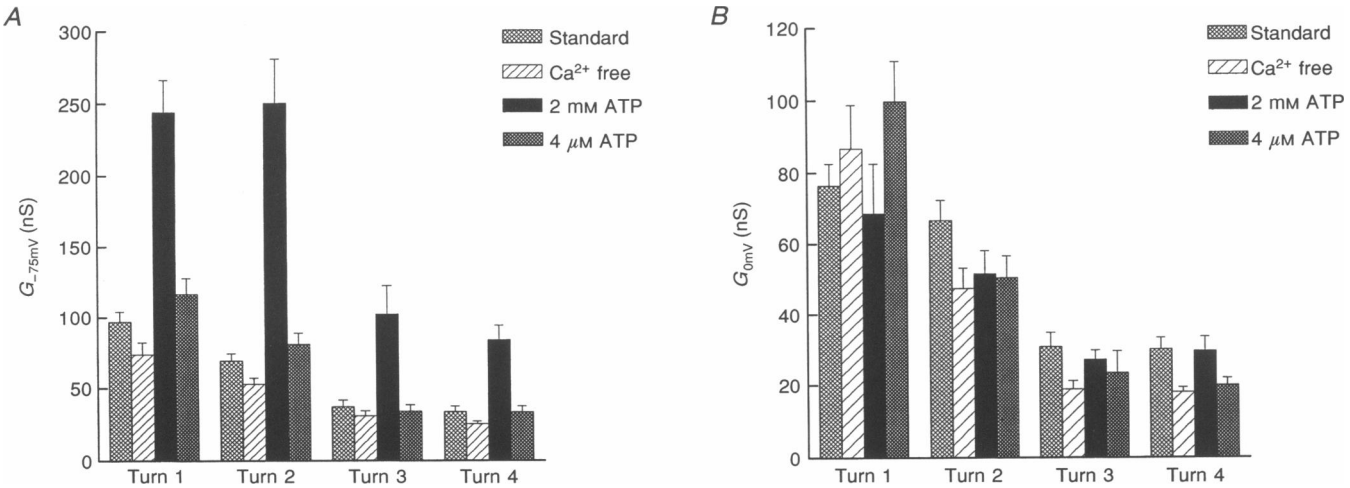

Figure 3. Slope conductance measured during the sequential superfusion of standard solution, Ca^{2+}-free solution and 2 mM ATP-containing, Ca^{2+}-free or 4 μM ATP-containing, Ca^{2+}-free solution for a total of 129 OHCs taken from the four turns of the cochlea

Each bin represents the mean ± S.E.M. of 10–37 recordings. *A*, slope conductance measured about −75 mV (G_{-75mV}). *B*, slope conductance measured about 0 mV (G_{0mV}).

background conductance gradient was maintained, from 25·0 ± 1·9 nS in the apex to 73·8 ± 8·2 nS in the base (Figs 1, 2 and 3*A*). The Ca^{2+} dependence of the slope conductances about 0 mV were more variable (Fig. 3*B*) due to changes in the shape of the *I–V* relationships of a number of cells. For example, fourteen out of sixty-six cells from turns 3 and 4 showed small increases in conductance about both 0 and −75 mV (Fig. 1, turn 4, and Fig. 2), while twelve out of twenty-six turn 1 OHCs and four out of thirty-seven turn 2 OHCs showed increases in slope conductance at 0 mV due to an unmasking of an outwardly rectifying conductance (Fig. 2, turn 1). The changes in slope and shape of the *I–V* relationships had a time course varying from 10 s to several minutes, presumably reflecting variation in initial OHC intracellular Ca^{2+} levels and the rate of decrease of $[Ca^{2+}]_i$ known to occur in the absence of external Ca^{2+} (Ashmore & Ohmori, 1990).

ATP-activated conductance

In OHCs voltage clamped at −60 mV, ATP caused the rapid onset (< 1 s) of sustained but reversible inward currents, whose amplitude was dependent upon OHC position in the cochlea (Fig. 1). Maximum ATP-gated currents (2 mM ATP) increased from a mean of −1·44 ± 0·19 nA in turn 4 OHCs to −3·99 ± 0·56 nA in turn 1 OHCs (Fig. 4). The significant variation in ATP-gated inward current across the different cochlear turns was also apparent with the lower concentration of ATP (4 μM), which still produced substantial responses in OHCs originating from the basal region

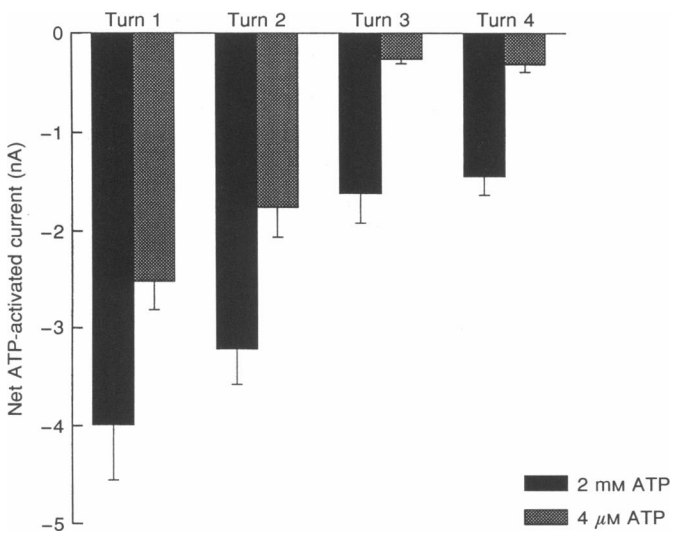

Figure 4. Steady-state inward current responses to 2 mM and 4 μM ATP-containing, Ca^{2+}-free solutions

Each bin represents the mean net ATP-activated current (V_h, −60 mV) measured immediately before the voltage ramp used for the determination of slope conductance. The comparison of the ATP-gated currents was made from 10–37 observations per cochlear turn. Error bars indicate S.E.M.

(−2·52 ± 0·30 nA in turn 1), whereas apical turn OHC responses were minimal (−0·32 ± 0·08 nA). Mean V_z in OHCs from all turns in 2 mM ATP was −24·4 ± 1·2 mV, while 4 μM ATP elicited significantly greater shifts in the basal turns (+25 mV) than in the apical turns (+10 mV). The ATP-gated currents were sustained with no indication of desensitization (up to 30 s); however, with 2 mM ATP some basal turn cells exhibited additional slower onset kinetics, which may reflect secondary conductance changes due to slow electro-osmotic volume loading as previously described by Housley *et al.* (1995*a*). The ATP-activated conductances were reversible with washout in the Ca^{2+}-free solution, with the exception that six out of ten turn 1 and four out of sixteen turn 2 OHCs exposed to 2 mM ATP lysed subsequent to obtaining the required *I–V* records; a consequence of the extremely high ATP-activated conductances and small volumes of these cells.

The conductance about −75 mV in the presence of 2 mM ATP increased significantly from 83·8 ± 10·1 nS in turn 4 OHCs to 244·0 ± 22·1 nS in turn 1 OHCs. This represented an increase of 330% over the background conductance under Ca^{2+}-free conditions for OHCs from all turns of the cochlea (Fig. 3*A*). Thus the available ATP-activated conductance paralleled $G_{K,n}$ irrespective of cell location.

The ATP-gated current records were determined by subtraction of the *I–V* relationship under Ca^{2+}-free conditions from the equivalent record obtained during exposure to ATP in Ca^{2+}-free solution (Fig. 2, traces labelled ATP). These subtracted ATP-gated current records displayed considerable inward rectification and reversal potentials close to 0 mV as previously reported (Nakagawa *et al.* 1990; Housley *et al.* 1992). The 2 mM ATP-activated conductance, measured about −75 mV, ranged from a minimum of 2·1 nS in a turn 4 OHC to a maximum of 375·2 nS in a turn 2 OHC (Fig. 5*A*), with mean values from 71–60 nS at the apex to 166–195 nS in the basal turns (Fig. 6*A*). ATP-activated conductances in the presence of 4 μM ATP showed a similar basal turn bias but ranged between 5% (apical OHCs) and 27% (basal OHCs) of the maximum ATP-activated conductance available (Figs 5*B* and 6*A*). The average ATP-activated conductance recorded about 0 mV for either 2 mM or 4 μM ATP was reduced to less than 15% of that about −75 mV due to inward rectification (Fig. 6*B*). The variance of these data reflects changes in the shapes of the *I–V* relationships about 0 mV during exposure to ATP, including incomplete rectification (Fig. 2, turn 2, trace 3).

DISCUSSION

The principal finding of this study was the increase in expression of the ATP-activated conductance in OHCs in the basal region of the cochlea. In addition, by studying OHCs isolated from known regions of the cochlea, we were able to confirm the earlier postulate that a position-dependent increase in the background membrane conductance exists towards the high frequency encoding region, which was based on a correlation between cell length and cochlear

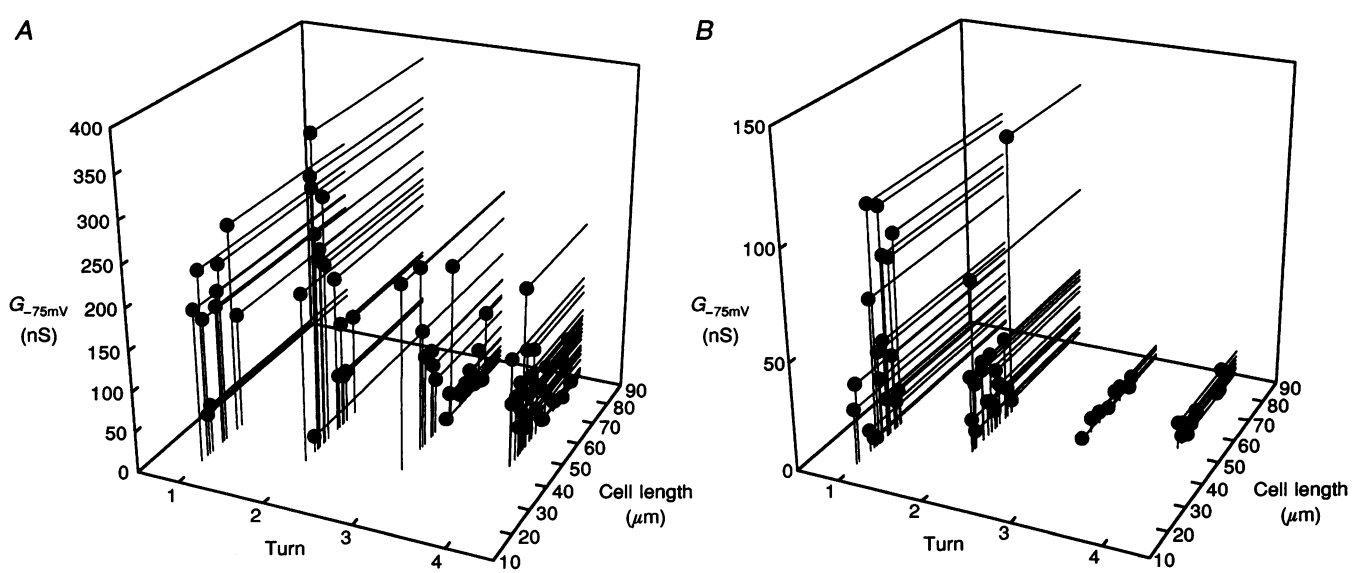

Figure 5. Comparison of the net ATP-activated conductance with cochlear turn and OHC length

A, net 2 mM ATP-activated conductance about −75 mV (G_{-75mV}) was greatest in the small basal turn OHCs and least in the largest apical turn OHCs. Variability in OHC length was greatest in turns 3 and 4. Data for 2 mM ATP-activated responses were calculated from 10–26 recordings per cochlear turn. *B*, net 4 μM ATP-activated conductance was greatest in turn 1 and diminished towards the apically located OHCs. Data for 4 μM ATP-activated responses were calculated from 10–18 recordings per cochlear turn.

origin (Housley & Ashmore, 1992). No previous data on basal turn OHC membrane conductances were available apart from a limited number of short OHCs reported in this previous study.

Our results also showed that the Ca^{2+} dependence of the negatively activated OHC K^+ conductance ($G_{K,n}$) (Housley & Ashmore, 1992) was approximately 30% *in vitro*. The current records at potentials positive to −40 mV suggest that a TEA-sensitive outwardly rectifying K^+ conductance ($G_{K,TEA}$), previously described in OHCs (Housley & Ashmore, 1992; Mammano, Kros & Ashmore, 1995; Mammano & Ashmore, 1995), is also modulated by intracellular Ca^{2+}. Both $G_{K,n}$ and $G_{K,TEA}$ are expressed in OHCs from all turns of the cochlea. The development of distinct outward rectification in the *I–V* relationship for turn 1 OHCs at potentials positive to approximately −40 mV under Ca^{2+}-free conditions (Fig. 2, turn 1) suggests that the $G_{K,TEA}$ conductance exhibits Ca^{2+}-dependent modulation of its voltage dependence, as previously described for similar K^+ conductances (Barrett, Magleby & Pallotta, 1982). Estimates of OHC input conductance recorded *in situ* from third row turn 3 and 4 OHCs (Mammano & Ashmore, 1995) are considerably lower than our measurements from OHCs isolated from these turns, presumably reflecting lower intracellular Ca^{2+} levels.

The reduction in conductance under Ca^{2+}-free conditions suggests that mechanisms regulating intracellular Ca^{2+} in OHCs *in vivo*, as recently proposed for the cholinergic efferent receptor mechanism of OHCs (Sridhar, Liberman, Brown & Sewall, 1995), and P2Y receptors (Nilles, Järlebark, Zenner & Heilbronn, 1994) may have a significant influence on membrane filtering characteristics, particularly in the more basal turns. Because $G_{K,n}$ is modulated by $[Ca^{2+}]_i$ and is greatest in the basal turns, the membrane time constant of the turn 1 and turn 2 OHCs was significantly increased when the external Ca^{2+} levels were lowered (Table 1).

While we cannot exclude the possibility that P2Y (G-protein coupled) receptors contributed to the ATP responses, this appears unlikely given the rapid onset of the ATP-gated current and the longer latency ATP-induced changes in OHC $[Ca^{2+}]_i$ attributed to P2Y receptors (Ashmore & Ohmori, 1990; Nilles *et al.* 1994). Additionally, Ca^{2+} activation of the background conductances would contribute less than a 30% increase, whereas the ATP-activated conductances were approximately 3 times larger in all turns and were rapidly reversible with washout, thereby obviating P2Y receptor influence.

Position-dependent variation in P2X receptor expression was evident from both the variation in ATP-gated current in OHCs isolated from the different regions of the cochlea and the associated ATP-activated slope conductances. The direct measurement of ATP-gated inward current was minimum in turn 4 and maximum in turn 1 for both the 2 mM and 4 μM ATP experiments (Fig. 4). This finding suggests that the greatest number of ATP-gated ion channels occurred on OHCs from the basal turn and this was supported by analysis of the net 4 μM ATP-activated conductances about −75 mV (Fig. 6*A*). The larger mean conductance exhibited by turn 2 OHCs than by turn 1 OHCs for 2 mM ATP may reflect a greater susceptibility to secondary effects of electro-osmotic cell volume loading (Housley *et al.* 1995*a*) by turn 1 OHCs. The non-physiological concentration of ATP

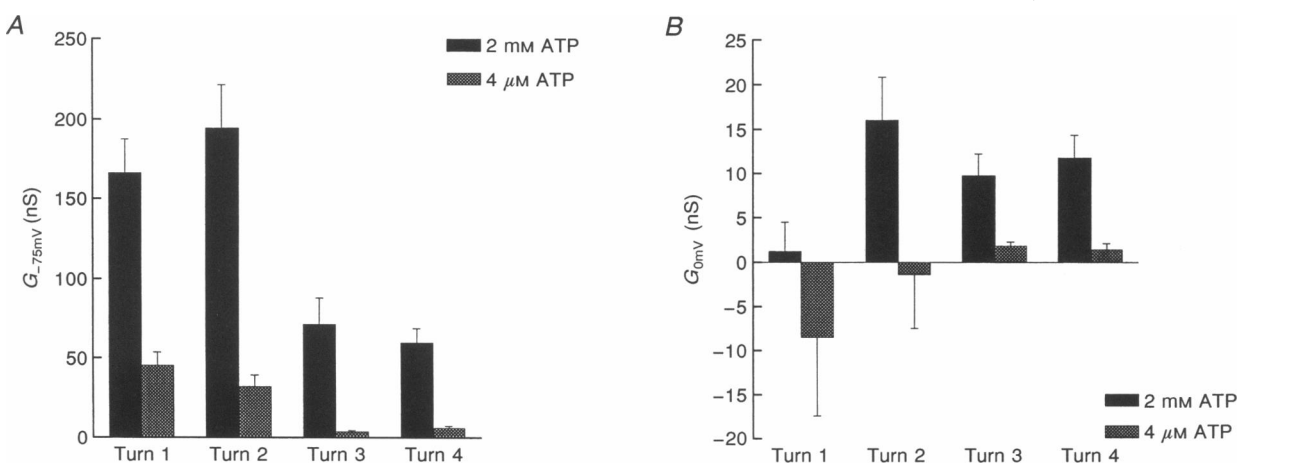

Figure 6. Comparison of net ATP-activated conductance between turns

A, net ATP-activated conductance about −75 mV was obtained by subtracting the corresponding conductance in the preceding Ca^{2+}-free solution from that obtained under the ATP-containing, Ca^{2+}-free condition. The mean 2 mM ATP-activated conductance was greatest in the more basal turns, and at the lower concentration (4 μM) the response was largest in turn 1. *B*, net ATP-activated conductance about 0 mV. The reduced slope conductances about 0 mV illustrate the substantial reduction in membrane conductance due to the strong inward rectification of the ATP-activated conductance. Each bin represents the mean ± S.E.M. of 10–26 recordings.

was applied to enable a semi-quantitative analysis of the number of ATP-gated ion channels on OHCs by maximally activating the P2X receptor conductance.

Given the average of 166 nS of maximum available ATP-activated conductance for turn 1 OHCs compared with only 60 nS for turn 4 OHCs, an estimated 16500 ATP-gated ion channels may be present on the stereocilia (Thorne & Housley, 1996) of basal turn OHCs compared with only 6000 on apical turn cells (based on an ATP-gated ion channel unitary conductance of 10 pS at −70 mV; after Lin, Hume & Nuttall, 1993). Estimates for the surface area of OHC stereocilia of 314 and 94 μm^2 for the apical and basal turn cells, respectively (based on published data for guinea-pig OHCs of 100 stereocilia, diameter 200 nm, average length 5 μm at the apex and 1·5 μm at the base, after Wright, 1984; Pickles, 1988), indicates that ATP-gated ion channel densities may approach 180 channels μm^{-2} on basal turn OHC stereocilia, compared with fewer than 20 channels μm^{-2} on stereocilia of apical turn OHCs. This may be compared (see Hille, 1992) with the density of ion channels in other tissues, such as Na^+ channels in rabbit vagus neurons (110 channels μm^{-2}) and bovine chromaffin cells (1·5–10 channels μm^{-2}) and *Torpedo* neuromuscular junction acetylcholine receptor density (10000 receptors μm^{-2}).

The ATP-activated conductance, localized to the stereocilia (Housley *et al.* 1992; Mockett *et al.* 1994; Thorne & Housley, 1996) would depolarize the OHCs, acting as an electrical shunt to short-circuit the mechano-electrical transduction (MET) current which passes down the stereocilia from stretch-gated ion channels associated with the tip-links of the stereocilia (Hudspeth, 1989). In OHCs the transduction conductance is estimated at approximately 5 nS, based on the presence of only a few 100 pS MET channels associated with the tip-links of the stereocilia (Torre, Ashmore, Lamb & Menini, 1995). Thus the maximum possible ATP-activated non-selective cation conductance exceeds the maximum MET conductance by nearly two orders of magnitude. The present study highlighted the sensitivity of OHCs to extracellular ATP, with low micromolar levels producing large changes in conductance in basal turn OHCs. Responses to 40 nM ATP have been reported in OHCs (Housley *et al.* 1992), presumably reflecting threshold modulation of the substantial number of ATP-gated channels which we have identified here. Thus endogenous ATP, present in low nanomolar concentrations in the endolymphatic compartment even under quiescent conditions (Muñoz *et al.* 1995*a*), may have a significant impact on the MET potential. The MET potential is known to drive OHC electromotility, which underlies the active mechanical amplification of the standing wave in the cochlea responsible for the sensitivity and frequency discrimination of hearing (for reviews see Dallos, 1992; Ashmore & Kolston, 1994).

Given the considerably greater electrical buffering of the more basal OHCs produced by the increased $G_{K,n}$, it is consistent with our model that there should be an increase in the number of ATP-gated ion channels in these cells if extracellular ATP is acting to disengage forward and reverse transduction in OHCs by reducing the −70 mV OHC membrane potential. This, along with an ATP-sensitive +80 mV endocochlear potential (EP) within the scala media, forms a 150 mV driving force for the OHC MET current (Ashmore, 1994).

Application of exogenous ATP into the scala media *in vivo* decreases the EP and hence the cochlear microphonic associated with OHC transduction (Muñoz *et al.* 1995*b*; Thorne & Housley, 1996). Thus the auditory nerve compound action potential is reduced. The ATP-induced drop in EP may be explained on the basis of the electrical shunt across the reticular lamina of the cochlea produced by current (largely carried by K^+ ions) entering the OHCs from the scala media through the ATP-gated ion channels and exiting via the basolateral K^+ conductances. Interestingly, ATP-gated ion channels are localized to the apical surface of neighbouring inner hair cells and Hensen cells (Housley *et al.* 1993; Sugasawa *et al.* 1996*a*, *b*), providing additional shunt paths across the reticular lamina for the ATP-mediated fall in EP. The present data suggest that the basal turn OHCs would contribute a significant proportion of this shunt conductance. No data are currently available regarding a similar positional bias in the ATP-activated conductances of inner hair cells or Hensen cells.

The actions of extracellular ATP in the cochlea are complicated and involve a number of different P2 receptor pathways at different sites (Kujawa, Erostegui, Fallon, Crist & Bobbin, 1994; Liu *et al.* 1995; Mockett *et al.* 1995; Thorne & Housley, 1996). It is likely that the site of action of the P2X receptor mechanism studied here on the endolymphatic face of the OHCs would limit OHC excitation under conditions where the extracellular ATP level becomes elevated. Given the short (< 20 ms) latency of the OHC ATP-gated ion channels (Housley *et al.* 1992; Thorne & Housley, 1996), the kinetics of OHC responses to endolymphatic ATP are likely to be determined by the origin of the extracellular ATP and diffusion time to the OHCs. Given the lack of apparent desensitization, termination of the ATP response is likely to depend upon ATP hydrolysis by ectonucleotidases. Interestingly, EP falls rapidly during anoxia (Woolf, Ryan & Harris, 1986). Thus it may be proposed that under local transient ischaemia or during toxin- or sound-induced stress, ATP, possibly released from purine stores identified in the marginal cells of the stria vascularis (White, Thorne, Housley, Mockett, Billett & Burnstock, 1995), could be responsible for this decrease in EP. An ATP-mediated depolarization of the OHC membrane potential, coupled with a more global ATP-mediated fall in EP, would limit the driving force of forward and reverse transduction across the OHC membrane, uncoupling the active hearing process mediated by these cells, thereby contributing to temporary threshold elevations in hearing which may protect OHCs from damage.

Ashmore, J. F. (1994). The cellular machinery of the cochlea. *Experimental Physiology* **79**, 113–134.

Ashmore, J. F., Housley, G. D. & Kolston, P. J. (1992). Two control systems for the outer hair cell motor. *Advances in the Biosciences* **83**, 19–25.

Ashmore, J. F. & Kolston, P. J. (1994). Hair cell based amplification in the cochlea. *Current Opinion in Neurobiology* **4**, 503–508.

Ashmore, J. F. & Ohmori, H. (1990). Control of intracellular calcium by ATP in isolated outer hair cells of the guinea-pig cochlea. *Journal of Physiology* **428**, 109–131.

Barrett, J. N., Magleby, K. L. & Pallotta, B. S. (1982). Properties of single calcium-activated potassium channels in cultured rat muscle. *Journal of Physiology* **331**, 211–230.

Burnstock, G. (1981). Neurotransmitters and trophic factors in the autonomic nervous system. *Journal of Physiology* **313**, 1–35.

Burnstock, G. (1995). Current state of purinoceptor research. *Pharmaceutica Acta Helvetiae* **69**, 231–242.

Dallos, P. (1992). The active cochlea. *Journal of Neuroscience* **12**, 4575–4585.

Gordon, J. L. (1986). Extracellular ATP: effects, sources and fate. *Biochemistry Journal* **233**, 309–319.

Hamill, O., Marty, A., Neher, E., Sakmann, B. & Sigworth, J. F. (1981). Improved patch-clamp techniques for high-resolution current recording from cells and cell-free membane patches. *Pflügers Archiv* **391**, 85–100.

Hille, B. (1992). Counting channels. In *Ionic Channels of Excitable Membranes*, pp. 315–336. Sinauer, Sunderland, MA, USA.

Housley, G. D. & Ashmore, J. F. (1992). Ionic currents of outer hair cells isolated from the guinea-pig cochlea. *Journal of Physiology* **448**, 73–98.

Housley, G. D., Connor, B. J. & Raybould, N. P. (1995*a*). Purinergic modulation of outer hair cell electromotility. In *Active Hearing*, vol. 65, ed. Flock, Å., Ottoson, D. & Ulfendahl, M., pp. 221–238. Elsevier, Oxford.

Housley, G. D., Greenwood, D. & Ashmore, J. F. (1992). Localization of cholinergic and purinergic receptors on outer hair cells isolated from the guinea-pig cochlea. *Proceedings of the Royal Society* B **249**, 265–273.

Housley, G. D., Greenwood, D., Bennett, T., Luo, L. & Ryan, A. F. (1995*b*). Differential expression of P2x purinoceptors in inner ear tissues. *Proceedings of the Molecular Biology of Hearing and Deafness, Symposium*. Bethesda, MD, USA, *P* 91.

Housley, G. D., Greenwood, D., Bennett, T. & Ryan, A. F. (1995*c*). Identification of a short form of the P2xR1-purinoceptor subunit produced by alternative splicing in the pituitary and cochlea. *Biochemical and Biophysical Research Communications* **212**, 501–508.

Housley, G. D., Greenwood, D., Mockett, B. G., Muñoz, D. J. B. & Thorne, P. R. (1993). Differential actions of ATP-activated conductances in outer and inner hair cells isolated from the guinea-pig organ of Corti: A humoral purinergic influence on cochlear function. In *Biophysics of Hair Cell Systems*, ed. Duifhuis, H., Horst, W., van Dijk, P. & van Netten, S. M., pp. 116–123. World Scientific, Singapore.

Hudspeth, A. J. (1989). How the ear's works work. *Nature* **341**, 397–404.

Kujawa, S. G., Erostegui, C., Fallon, M., Crist, J. & Bobbin, R. P. (1994). Effects of adenosine 5′-triphosphate and related agonists on cochlear function. *Hearing Research* **76**, 87–100.

Lin, X., Hume, R. I. & Nuttall, A. L. (1993). Voltage-dependent block by neomycin of the ATP-induced whole cell current of guinea-pig outer hair cells. *Journal of Neurophysiology* **70**, 1593–1605.

Liu, J., Kozakura, K. & Marcus, D. C. (1995). Evidence for purinergic receptors in vestibular dark cell and strial marginal cell epithelia of the gerbil. *Auditory Neuroscience* **1**, 331–340.

Mammano, F. & Ashmore, J. F. (1995). Differential expression of outer hair cell potassium currents in the apical turns of the isolated cochlea of the guinea-pig. *Journal of Physiology* **485.P**, 30*P*.

Mammano, F., Kros, C. J. & Ashmore, J. F. (1995). Patch clamped responses from outer hair cells in the intact adult organ of Corti. *Pflügers Archiv* **430**, 745–750.

Mockett, B. G., Bo, X., Housley, G. D., Thorne, P. R. & Burnstock, G. (1995). Autoradiographic labelling of P_2 purinoceptors in the guinea-pig cochlea. *Hearing Research* **84**, 177–193.

Mockett, B. G., Housley, G. D. & Thorne, P. R. (1994). Fluorescence imaging of extracellular purinergic receptor sites and putative ecto-ATPase sites on isolated cochlear hair cells. *Journal of Neuroscience* **14**, 6992–7007.

Muñoz, D. J. B., Thorne, P. R., Housley, G. D. & Billett, T. E. (1995*a*). Adenosine 5′-triphosphate (ATP) concentrations in the endolymph and perilymph of the guinea-pig cochlea. *Hearing Research* **90**, 119–125.

Muñoz, D. J. B., Thorne, P. R., Housley, G. D., Billett, T. E. & Battersby, J. M. (1995*b*). Extracellular adenosine 5′-triphosphate (ATP) in the endolymphatic compartment influences cochlear function. *Hearing Research* **90**, 106–118.

Nakagawa, T., Akaike, N., Kimitsuki, T., Komune, S. & Arima, T. (1990). ATP-induced current in isolated outer hair cells of guinea pig cochlea. *Journal of Neurophysiology* **63**, 1068–1074.

Nilles, R., Järlebark, L., Zenner, H. P. & Heilbronn, E. (1994). ATP-induced cytoplasmic [Ca^{2+}] increases in isolated cochlear outer hair cells. Involved receptor and channel mechanisms. *Hearing Research* **73**, 27–34.

Pickles, J. O. (1988). Mechanisms of transduction and excitation in the cochlea. In *An Introduction to the Physiology of Hearing*, pp. 112–162. Academic Press, London.

Pujol, R., Lenoir, M., Ladrech, S., Tribillac, F. & Rebillard, G. (1992). Correlation between the length of outer hair cells and the frequency coding of the cochlea. In *Auditory Physiology and Perception*, ed. Cazals, Y., Demany, L. & Horner, K. C., pp. 45–52. Pergamon Press, Oxford.

Sridhar, T. S., Liberman, M. C., Brown, M. C. & Sewall, W. F. (1995). A novel cholinergic slow effect of efferent stimulation on cochlear potentials in the guinea pig. *Journal of Neuroscience* **15**, 3667–3678.

Sugasawa, M., Erostegui, C., Blanchet, C. & Dulon, D. (1996*a*). ATP activates non-selective channels and calcium release in inner hair cells of the guinea-pig cochlea. *Journal of Physiology* **491**, 707–718.

Sugasawa, M., Erostegui, C., Blanchet, C. & Dulon, D. (1996*b*). ATP activates a cation conductance and a Ca^{2+}-dependent chloride conductance in Hensen cells of the guinea-pig cochlea. *American Journal of Physiology* (in the Press).

Thorne, P. R. & Housley, G. D. (1996). Purinergic signalling in sensory systems. *Seminars in the Neurosciences* **8**, 233–246.

Torre, V., Ashmore, J. F., Lamb, T. D. & Menini, A. (1995). Transduction and adaptation in sensory receptor cells. *Journal of Neuroscience* **15**, 7757–7768.

WHITE, P. N., THORNE, P. R., HOUSLEY, G. D., MOCKETT, B. G., BILLETT, T. E. & BURNSTOCK, G. (1995). Quinacrine staining of marginal cells in the stria vascularis of the guinea-pig cochlea: a possible source of extracellular ATP? *Hearing Research* **90**, 97–105.

WOOLF, N. K., RYAN, A. F. & HARRIS, J. P. (1986). Development of mammalian endocochlear potential: normal ontogeny and effects of anoxia. *American Journal of Physiology* **250**, R493–498.

WRIGHT, A. (1984). Dimensions of the cochlear stereocilia in man and the guinea pig. *Hearing Research* **13**, 89–98.

Acknowledgements

This work was funded by the Health Research Council of New Zealand, the New Zealand Deafness Research Foundation, the New Zealand Lottery Grants Board and the Wallath Trust. We thank D. Greenwood for technical assistance and Dr M. Parkis for comments on this manuscript.

Author's email address

G. D. Housley: g.housley@auckland.ac.nz

Received 2 May 1996; accepted 11 October 1996.